CONTROL SYSTEMS LABORATORY

SEA CLUTTER SPECTRUM STUDIES USING

AIRBORNE COHERENT RADAR III

Report R-105

May, 1958

Contract DA-36-039-SC-56695
D/A Sub-Task 3-99-06-111

UNIVERSITY OF ILLINOIS · URBANA · ILLINOIS

"The research reported in this document was made possible by support extended to the University of Illinois, Control Systems Laboratory, jointly by the Department of the Army (Signal Corps and Ordnance Corps), Department of the Navy (Office of Naval Research), and the Department of the Air Force (Office of Scientific Research, Air Research and Development Command), under Signal Corps Contract DA-36-039-SC-56695, D/A Sub-Task 3-99-06-111."

SEA CLUTTER SPECTRUM STUDIES USING AIRBORNE COHERENT RADAR III

by

B. L. Hicks

N. Knable

J. J. Kovaly

G. S. Newell

J. P. Ruina

Report R-105

May, 1958

CONTROL SYSTEMS LABORATORY
UNIVERSITY OF ILLINOIS
URBANA, ILLINOIS
Contract DA-36-039-SC-56695
D/A Sub-Task 3-99-06-111

Numbered Pages: 31

TABLE OF CONTENTS

ABSTRACT

Coherent radar measurements can clarify the spectral properties of sea clutter as compared to noncoherent observations where, for example, the asymmetry of the clutter spectra and the sense of motion of scatterers cannot be observed. Coherent radar measurements can also yield new means of characterizing the properties of wind waves, especially the distribution in range and azimuth of the particle velocities of waves and of the materials associated with white caps. The Control Systems Laboratory has observed sea clutter with a coherent radar. These studies are described in the present paper and illustrate the two areas of usefulness of coherent radar data.

Sea clutter was observed off the coast of New England with an airborne, coherent, X-band radar. Sea state data was derived from hindcasts and local observations to provide a characterization of the sea surface responsible for the clutter.

Frequency B-scope displays and power spectra of the clutter were calculated from the observational data. The B-scope displays indicate again, as in earlier CSL measurements made off the coast of Florida, that the upwind edge of the clutter spectrum is smooth for all wind speeds observed but that the downwind edge, for sea state 3 or above, is broadened in an irregular fashion as a function of range. This irregular broadening implies a considerable variability, from patch to patch, in the downwind side of the probability distribution of velocity of scatterers on the sea surface.

The coherent clutter spectra were calculated by averaging in range over an interval of 3750 ft. These spectra are equivalent to the average probability distribution of scatterer velocities on this patch of sea surface, and the width at half power of the coherent clutter spectrum is proportional, for reasonable assumptions, to width at half maximum of the probability distribution of scatterer velocities. The variation of the latter width, Δ_o, with sea state can be represented by the equation (expressed in consistent units)

$$\Delta_o = 11\, H_{1/3}\, T_m^{-1}$$

where the numerical factor is dimensionless, $H_{1/3}$ is the significant wave height, and T_m is the period corresponding to the maximum of the energy spectrum for the waves, plotted as a function of frequency. This equation fits the experimental data within about 10 o/o for bandwidths in the range two to five knots and wind speeds in the range eight to nineteen knots. The bandwidth of the clutter was also found to be approximately proportional to the wind speed. Theoretical calculations indicate that less than one-half of the observed average width of the clutter spectra can be attributed to the distribution of (orbital) particle velocities of the waves. The distribution of drift and white cap velocities presumably contribute the other one-half or more of the observed width of the spectra. The spectra are asymmetric for the higher sea states, and these also produce the irregular downwind broadening of the "B" display.

The variation of clutter bandwidth with the depression angle of the radar did not seem to be too well defined nor reproducible. For

some runs at high sea states the bandwidth was observed to be from one-half to one knot wider for a depression angle of 10° than for a depression angle of 1°, but in one case the bandwidth decreased by two knots for a change of depression angle from 2.5 to 6°. The small width of the clutter at low sea states and small depression angles that was observed at Key West seems to be verified by the newer observations. Clutter bandwidths observed when the radar was looking crosswind are larger relative to the bandwidths observed when the radar was looking up- or down-wind than would be predicted from a $\cos^2$ beam shape of the wave spectrum.

In five of the 200 or so samples of clutter data recorded, the "B" displays showed a downwind displacement of the clutter spectrum by as much as seven knots, which persisted for one or two seconds. The origin of these anomalies has not been fixed. On several other occasions the clutter spectrum of a rain cloud was observed simultaneously with the clutter spectrum of the sea return.

I. Introduction

Two previous CSL reports[1,2] described results obtained from measurements of the doppler frequency spectrum of sea clutter with a pulsed, X-band, airborne, phase coherent radar. Coherence was obtained by use of an echo box whose ringing time limited the useful range of this system to about 8000 yards. These experiments were made off the southern coast of Florida where the water was comparatively calm.

Additional measurements were made in the fall of 1954 off the southern coast of New England and are reported here. Our search of the open literature yielded no other sea clutter data measured with a coherent radar. These measurements extend the scope of the earlier ones by

1. including rougher sea conditions;
2. providing data for longer ranges or smaller depression angles;
3. supplementing the radar data with data on winds and waves obtained from the U. S. Navy Hydrographic Office.

The characteristics of sea return are determined by the nature of the sea surface. We feel, therefore, that the correlation of radar measurements with simultaneous quantitative measurement of sea surface conditions would be extremely significant. It was one of the prime purposes of our experiments to obtain data for such a correlation. However, hurricanes and generally unfavorable weather conditions at the time of our experiments limited the scope of both the radar and the

---

[1] CSL Report R-27 (1952) (Secret).

[2] CSL Report R-36 (1953) (Confidential).

oceanographic measurements.

We are indebted to the Woods Hole Oceanographic Institute for their help in making oceanographic measurements. We also wish to acknowledge the considerable assistance given to us by the U. S. Navy Hydrographic Office which provided us with accurate hindcast data and the professional services of two oceanographers for a period of several weeks.

II. Experimental Procedure

1. Method of Observation

The CSL data were obtained during flights along the courses shown in Fig. 1. Most of the flights were along the East-West course between Nantucket and Montauk Point. The courses were chosen to be as far seaward as was practicable with Atlantic Air Defense Identification Zone (ADIZ) restrictions. The aircraft was flown at an air speed of about 150 knots. The radar antenna was fixed in the direction of the ground track, by setting the antenna azimuth for maximum doppler frequency shift of the radar return. The radar return from a 250 ft. range interval was gated and recorded on tape for spectrum analysis in the laboratory. The aircraft flew the distance corresponding to the length of the range gate in approximately one second. Values of some of the other parameters were

position of the range gate	1,000 - 22,000 yds.
aircraft altitude	500 - 2,500 ft.
depression angle*	0.4 - 20°

---

* Defined by the radar altitude and the range of the patch being observed on the ocean.

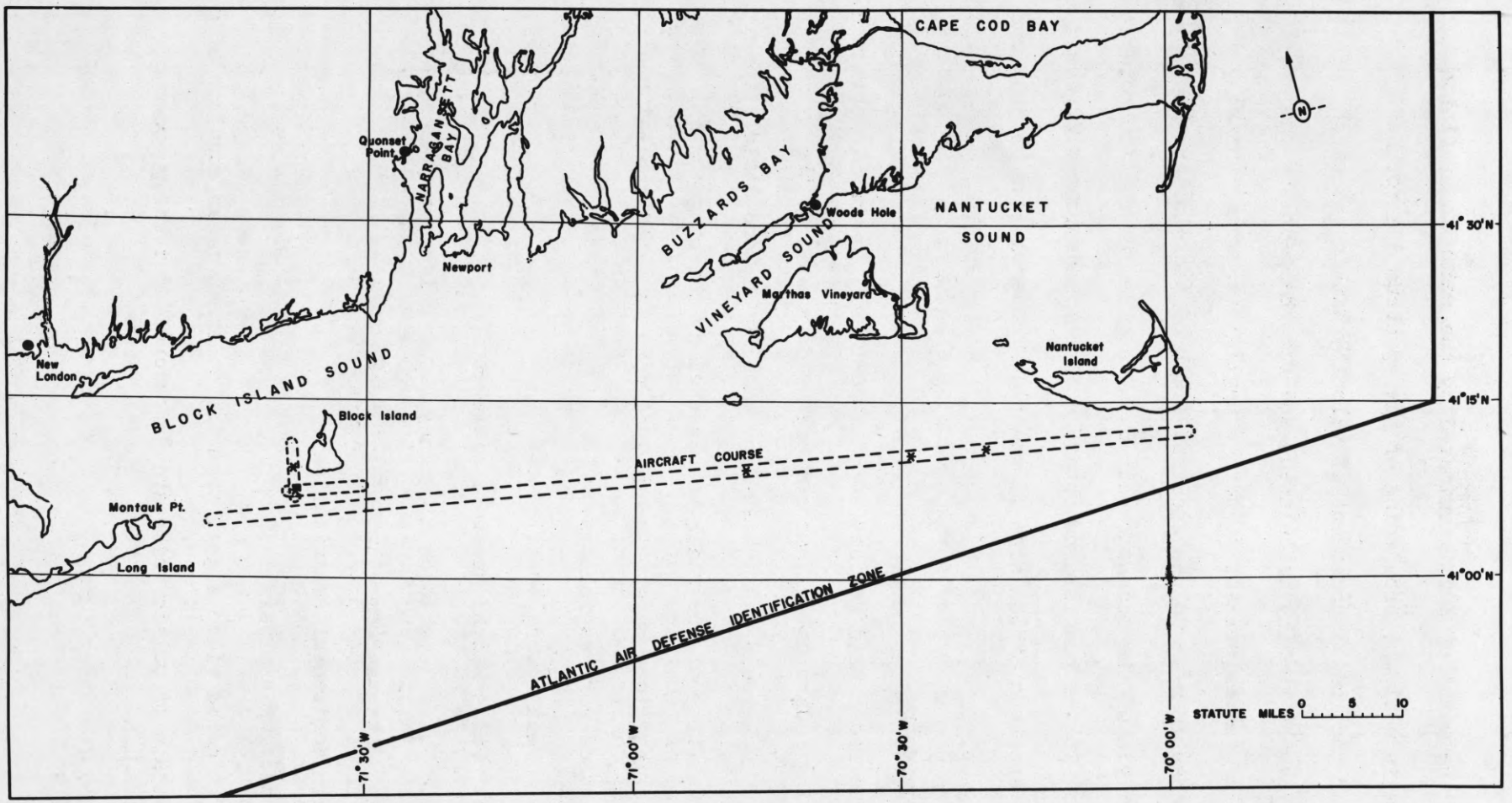

FIG. I MAP OF EXPERIMENTAL AREA

Since the patch of sea illuminated by the radar is of finite size, there is a slight broadening of the spectrum due to the variation of the radial component of velocity within the patch. This broadening can be readily calculated, and for the geometry and parameters of our experiment it adds a negligible amount (usually much less than 10 o/o) to the spectral width of the clutter.

The origin of the oceanographic data is given in the footnotes to Table I. It was possible to obtain a direct measurement of the ocean wave spectrum at the site of the radar observations on just one day, September 24.

2. Equipment

The radar used was developed at CSL from components obtained from existing radars as well as components developed by the laboratory. Coherence was achieved by means of a Coho-Stalo system. Adequate stability of the radar was assured by checking its performance in flight on stationary land targets. The nominal radar characteristics were as follows:

a. Peak Power: 40 kilowatts

b. Pulse Width: one-half microsecond

c. Pulse Repetition Frequency: 2000 pulses per second

d. Antenna Beam Width: 1.5°(APS 23 Antenna)

e. Horizontal Polarization

3. Spectrum Analysis

The gated video signal from the coherent radar consists of a modulated train of pulses which are "stretched" for the purpose of

amplification. The spectrum of the stretched pulse train[3] appears both near the pulse repetition frequency and its harmonics.* To obtain complete information concerning the spectrum of the return it is sufficient to examine the spectrum over a frequency interval equal to one-half the pulse repetition frequency and extending above or below any harmonic line. The observed doppler frequency will either increase or decrease as the velocity of the scatterer increases depending on whether the particular sideband observed is the upper or lower sideband of a harmonic line. We refer to the two types of spectra as "direct" and "inverted". In Plate II, the "A" display for Sample No. 140 is an example of a normal spectrum, and the "A" display for Sample No. 171 is an example of an inverted spectrum.

Two methods were used to determine which type of spectrum was being observed: first, by sector scanning the antenna about the ground track and observing the doppler frequency of the return; second, by observing the doppler frequency variation when the range gate was decreased to short ranges, thereby decreasing the radial component of the clutter velocity. The two methods gave consistent results.

The signal, after pulse stretching, was recorded on tape for later analysis and also fed to a Rayspan unit.** The output of Rayspan was

---

[3] Lawson and Uhlenbeck, Threshold Signals, Vol. 24, Rad. Lab. Series, McGraw-Hill, Sec. 2.7.

* If $g(f)$ is the doppler clutter spectrum then the spectrum of the stretched pulse train has the form $\sum_n a_n g(|nf_o \pm f|)$ where f_o is the pulse repetition frequency.

** The Rayspan unit (Raytheon Spectrum Analyzer) consists of a bank of magnetostriction rods covering a bandwidth of 1000 cycles. Each filter is nominally 25 cycles wide. Rayspan scans the output of the filters in sequence by means of a rotating commutator.

displayed as the ordinate of a cathode ray tube display having a linear sawtooth synchronized with the Rayspan commutator. The principle limitations of Rayspan as a quantitative instrument for spectrum analysis are its poor frequency resolution and large variations in sensitivity in different parts of the frequency band. However, we found that Rayspan was useful for monitoring the spectrum in flight.

The analysis of the magnetic tape recordings of the sea clutter obtained on the flights was made with the apparatus shown in block form in Fig. 2. Recorded samples of sea clutter of 15 second duration were formed into loops for analysis. The results were displayed in two ways: by a graphical recorder which plotted power spectral density versus frequency (or velocity); and on a CRO, which was photographed, with time (zero to fifteen seconds), frequency, and power spectral density as the variables displayed on the y, x and z axes, respectively. Examples of these displays may be seen in Plates I to III.* The first or "A" display utilized five second smoothing while the second or "B" display used no smoothing. A short, high frequency tone was added on the sample loops to trigger the vertical sweep for the "B" display.

The bandwidth of the wave analyzer that was used as the narrow band selection filter in the apparatus was measured to be approximately 9 cycles; however, the "wow" of the tape recorder (0.3 o/o) limited the frequency resolution to about 12 cps.

Spectral analysis by means of a narrow band filter has two

---

* The plane speeds noted on the Plates are indicated air speeds.

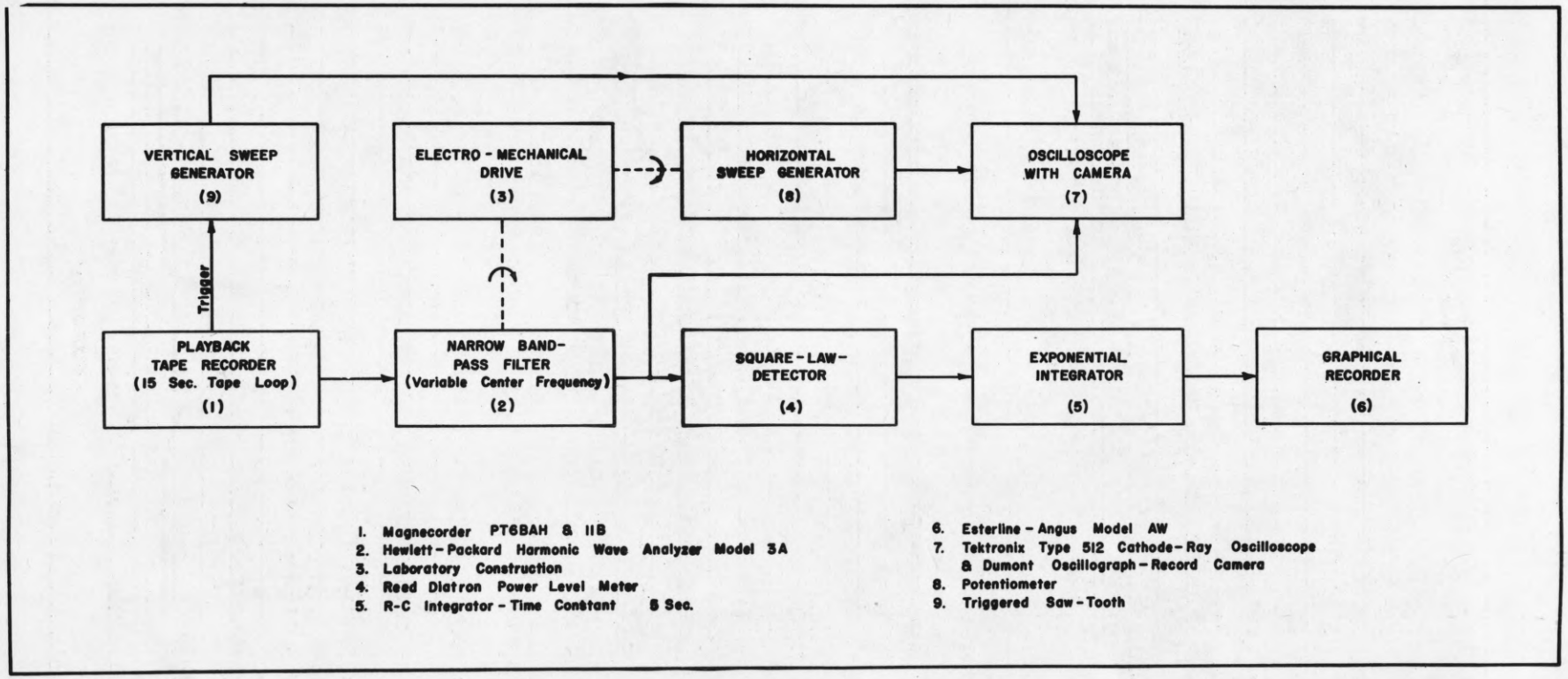

1. Magnecorder PT6BAH & 11B
2. Hewlett-Packard Harmonic Wave Analyzer Model 3A
3. Laboratory Construction
4. Reed Diatron Power Level Meter
5. R-C Integrator - Time Constant 5 Sec.
6. Esterline - Angus Model AW
7. Tektronix Type 512 Cathode-Ray Oscilloscope & Dumont Oscillograph - Record Camera
8. Potentiometer
9. Triggered Saw-Tooth

FIG. 2 BLOCK DIAGRAM OF POWER SPECTRUM ANALYZER

PLATE I

A Display

B Display

SAMPLE NO. 232
Sept. 23, 1954
Altitude - 500 ft.
Range - 1980 yds.
Depression - 4.84°
Wave height - 4.5 ft.
3 db bandwidth 163 cps

A/C 130 knots
20°
Wind
19 knots

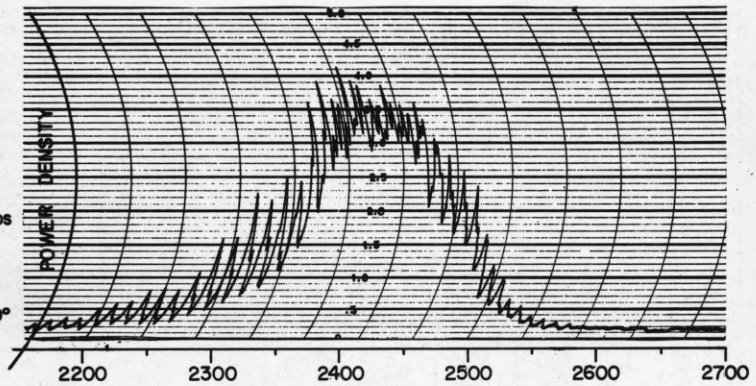

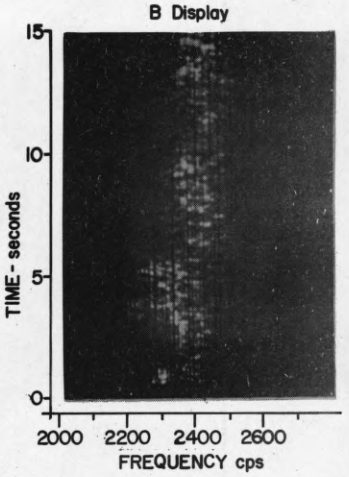

SAMPLE NO. 300
Sept. 25, 1954
Altitude - 1000 ft.
Range - 9030 yds.
Depression - 2.12°
Wave height - 4.5 ft.

A/C 160 knots
70°
Wind
19 knots

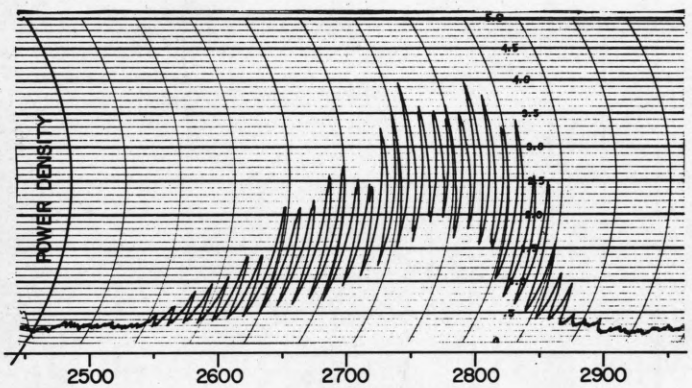

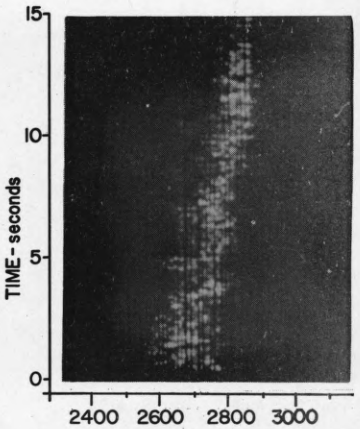

SAMPLE NO. 262
Sept. 24, 1954
Altitude - 1000 ft.
Range - 13,050 yds.
Depression - 1.46°
Wave height - 2.0 ft.
3 db bandwidth - 82 cps

WIND
9 knots
80°
A/C 144 knots

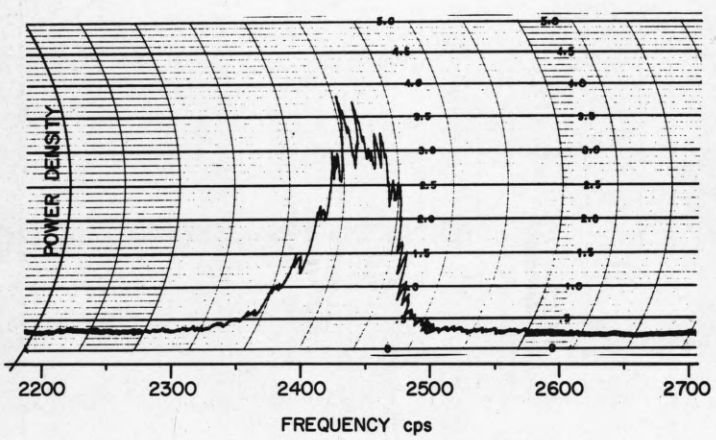

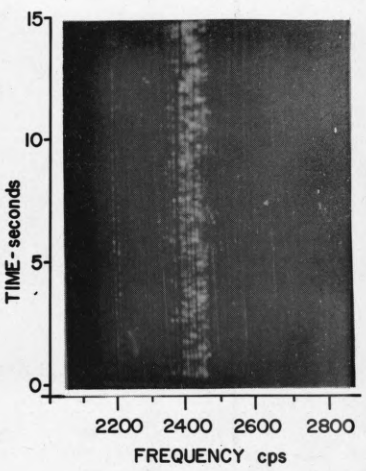

PLATE II

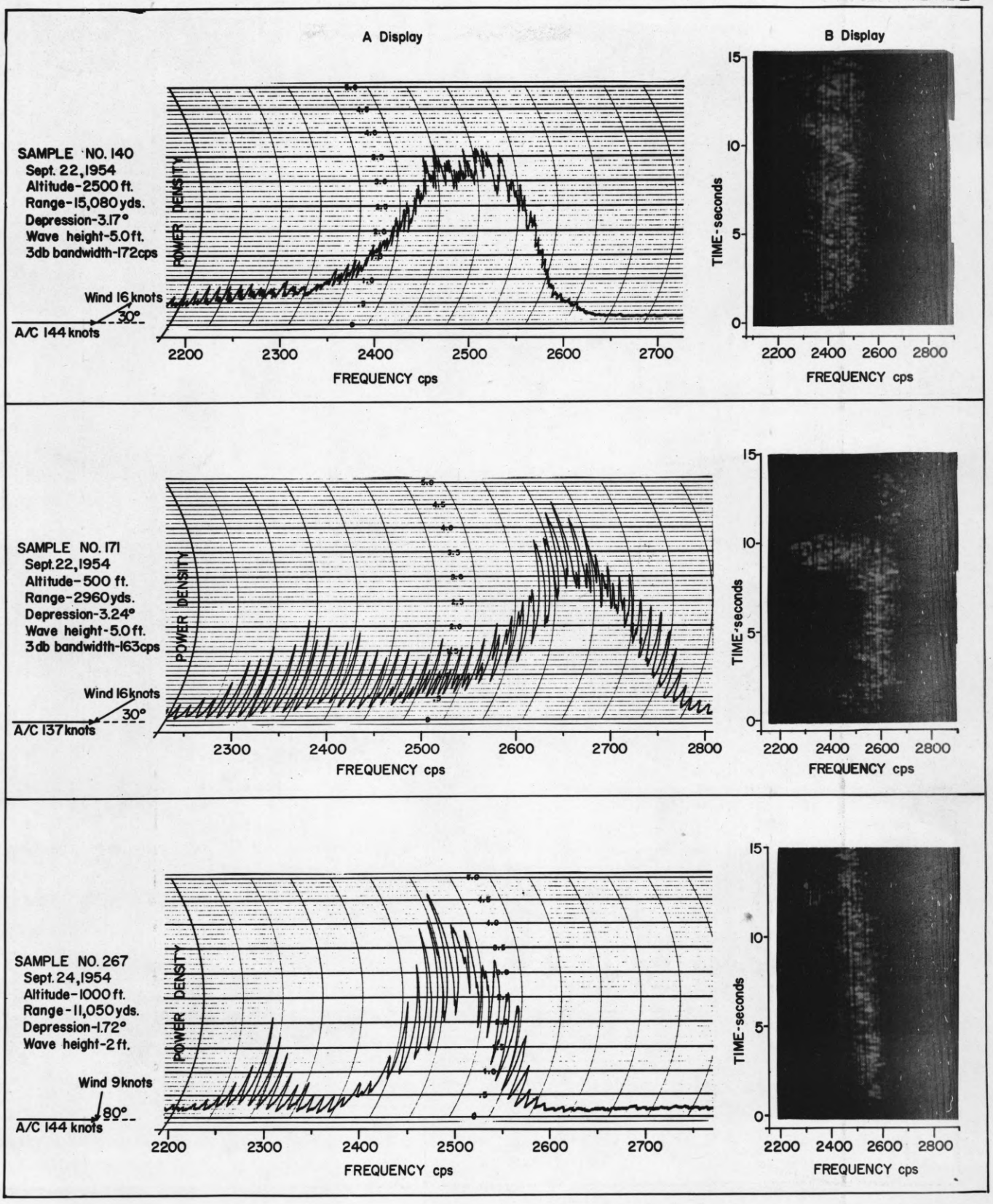
A Display
B Display
SAMPLE NO. 140
Sept. 22, 1954
Altitude-2500 ft.
Range-15,080 yds.
Depression-3.17°
Wave height-5.0 ft.
3db bandwidth-172cps
Wind 16 knots
30°
A/C 144 knots
POWER DENSITY
FREQUENCY cps
TIME-seconds
SAMPLE NO. 171
Sept. 22, 1954
Altitude-500 ft.
Range-2960 yds.
Depression-3.24°
Wave height-5.0 ft.
3db bandwidth-163cps
Wind 16 knots
30°
A/C 137 knots
SAMPLE NO. 267
Sept. 24, 1954
Altitude-1000 ft.
Range-11,050 yds.
Depression-1.72°
Wave height-2 ft.
Wind 9 knots
80°
A/C 144 knots

PLATE III

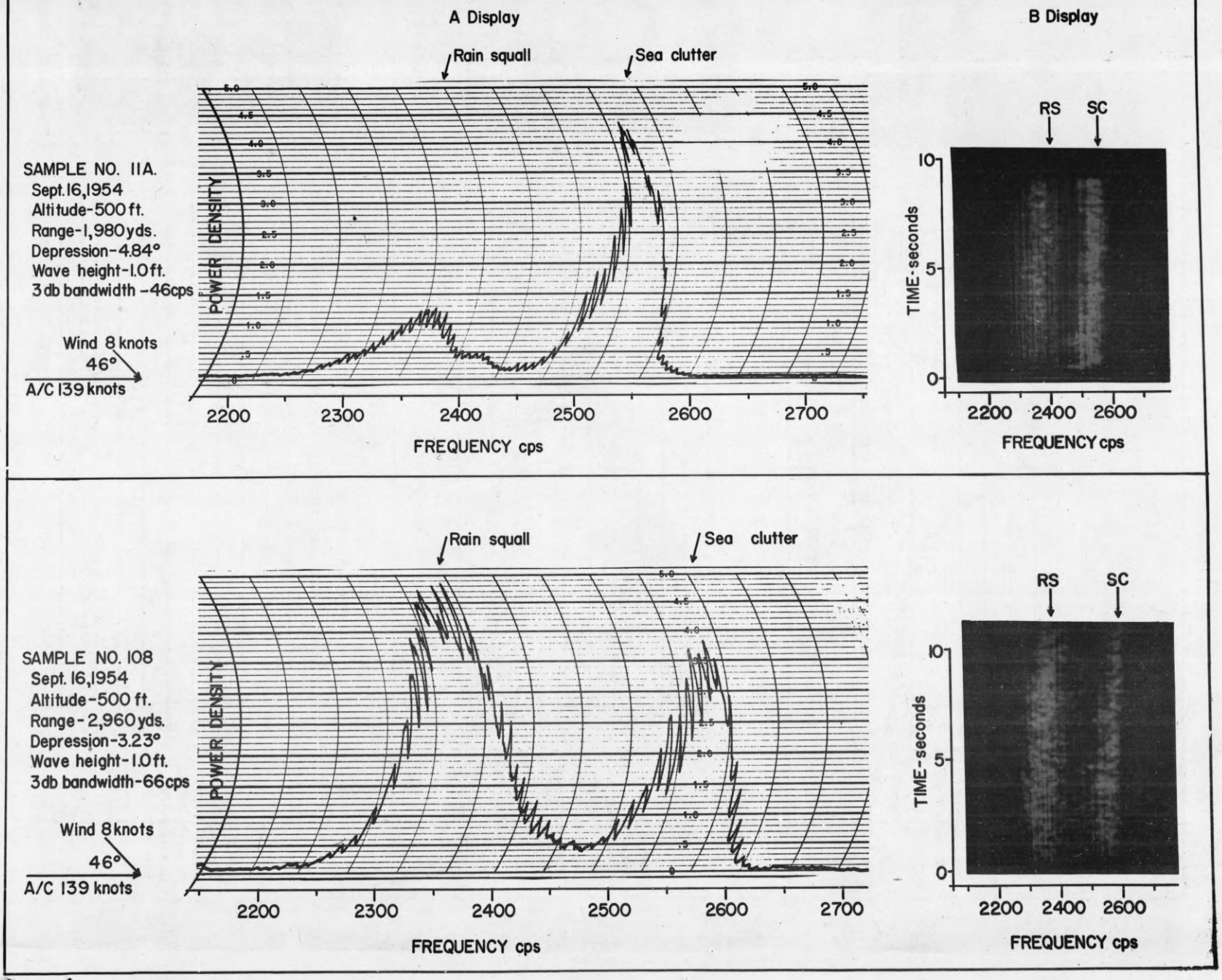
A Display
B Display
Rain squall
Sea clutter
SAMPLE NO. 11A.
Sept. 16, 1954
Altitude-500 ft.
Range-1,980 yds.
Depression-4.84°
Wave height-1.0 ft.
3 db bandwidth -46 cps
Wind 8 knots
46°
A/C 139 knots
POWER DENSITY
FREQUENCY cps
RS
SC
TIME-seconds
SAMPLE NO. 108
Sept. 16, 1954
Altitude-500 ft.
Range-2,960 yds.
Depression-3.23°
Wave height-1.0 ft.
3db bandwidth-66 cps
Wind 8 knots
46°
A/C 139 knots

inherent sources of error. The first is the fluctuation of the power level reading. If Δf is the filter bandwidth and T is the integration time then the error is of the order of $1/\sqrt{\Delta fT}$, for $\Delta fT \gg 1$. The second is due to the finite frequency resolution of the filter. This error increases with filter bandwidth and is a function of the higher order derivatives of the spectrum measured. Increasing the filter bandwidth decreases the first error but increases the second. However, these inherent errors in the spectral measurements were found to be small compared to the overall experimental errors (standard deviations) listed in Table I.

III. Results

1. "B" Display

Since the "B" display photographs are obtained without any integration, they indicate the spectrum for each patch* illuminated by the radar but of course exhibit 15 different patches at 15 different times. For the samples which have a symmetrical "A" display spectrum, we find that the two borders of the "B" display, corresponding to the bandwidth as seen on the "B" displays, are both smooth. An example of this is shown in Plate I, Sample No. 262. Similar symmetrical spectra were always observed for low sea states when the radar was looking up- or down-wind. However, when the clutter was obtained looking upwind or downwind on rough waters, the border of the spectrum corresponding to

---

* Each patch contained only one to two ocean waves of average length for the sea states that existed during the flights. The "B" display therefore exhibits fluctuations from patch to patch.

the downwind-moving scatterers was rough* as shown in Plate II, Sample No. 140, and the "A" display is then unsymmetrical. This result, which was also found at Key West[2], suggests that one may consider X-band sea clutter, in the range of sea state that we observed, as coming from two sets of back scatterers. The first set have a symmetrical spectrum whose shape and bandwidth may be relatively insensitive to wind and sea conditions. These scatterers are likely to be those surface waves whose dimensions are of the same magnitude as the radiation wavelength (3.2 centimeters). The second set, which we presume to be connected with the whitecaps, has a spectrum displaced in the direction of the wind velocity, thereby causing the spectrum averaged in range to be asymmetrical. The roughness of the windward border of the "B" display photograph is then due to the uneven distribution of the whitecap areas on the sea surface that are illuminated by the radar.

The number and extent of the areas of whitecap, spray and foam can be estimated qualitatively from the wind speed.[4] For a Beaufort Number of 3 (7-10 knot wind) the crests are beginning to break, producing a few scattered whitecaps described as (scattered) "foamy crests", and there are a "few foamy ridges". For a Beaufort Number of 5 (17-21 knot wind) whitecaps appear "all over" the sea, "widely

---

* The roughness of the downwind edge was generally irregular for the New England measurements. The roughness had appeared to be periodic in the Key West measurements.[2] The roughness of the downwind edge of the "B" display was generally more noticeable when looking upwind rather than downwind.

[4] H. T. Seilkopf, Der Seewart 17, 210 (1956).

scattered spray" is beginning to show, and the wave ridges are foamy. Foam patches appear for slightly stronger winds. Beaufort Numbers 3-5 cover the range of sea states in our experiments. If we attribute backscattering of X-band radiation to breaking wave crests, to spray, and perhaps to foam we can then understand the irregular downwind broadening of the coherent clutter spectrum that increases with increase of sea state.

It is clear that semi-quantitative analysis of "B" displays can yield considerable information about the properties of a patch of sea surface several hundred feet square. Moderate acceleration of the radar platform does not destroy this information in the "B" displays.

2. "A" Display

(a) Selection of Samples

The 95 samples used for the "A" display data were selected from the more than 200 recorded samples by rejecting those samples taken when the aircraft acceleration in the 15 second interval was large enough to change the width of the spectrum for the "A" display more than other sources of error in the width. Sample 300 in Plate I shows an example of the broadening and also of the large oscillations in the "A" display which are produced when a sample such as shown in the corresponding "B" display was recorded while the plane was accelerating. The half power spectral bandwidth of the "A" display for each sample selected was measured and the average bandwidth of all the samples selected from each flight were averaged and are listed in Table I together with the Hydrographic Office hindcast wave data for each day of flight. In interpreting these "A" display results, we should

Mean Bandwidth* at Half-power	Δ	** Significant Wave Height	** Wind Speed	** Wave Energy	Depression Angle		Number of Samples Used	Date of Observation	Flight Number
(cycles/sec)	(knots)	(ft)	(knots)	(ft^2)	(degrees)				
up or down wind					Min.	Max.			
67 ± 7^a	2.09 ± 0.22^a	4.0	15	4	2.8	10.7	3	9-7-54	2
70 ± 9^b	2.19 ± 0.28^b	1.0	8	0.01	2.5	10.7	10	9-16-54	4
76 ± 5	2.38 ± 0.16	1.5	10	0.08	1.9	3.2	3	9-21-54	5
79 ± 10	2.47 ± 0.32	2.0	9^c	0.23^c	1.1	13	17	9-24-54	8
121 ± 10	3.78 ± 0.32	4.5	19	6.0	0.9	13	5	9-25-54	9
124 ± 17	3.88 ± 0.53	4.5	19	6.0	0.4	20	25	9-23-54	7
157 ± 17	4.91 ± 0.53	5.0	16	6.7	0.5	16	19	9-22-54	6
cross wind									
95 ± 17	2.97 ± 0.53	4.5	19	6.0	0.9	13	13	9-25-54	9

See footnotes on next page.

TABLE I

Footnotes for Table I

* The mean bandwidth at half-power is the mean of the values measured for the range of depression angles shown in columns 6 and 7 of the table. This mean is equal, within experimental error, to the value of the clutter bandwidth at half-power for a depression angle of 4°. The variation of bandwidth with depression angle is discussed later.

** Data supplied by the U. S. Navy Hydrographic Office for the area near 41° 25' N, 71° 20' W.

- Significant wave height is the average height of the highest one-third of the waves. Values were derived by the Hydrographic Office from visual estimates reported from ships in the area.

- Values of the wind velocity were obtained by the Hydrographic Office reports by ships in the area.

- Values of the wave energy E were computed (hindcast) by the Hydrographic Office from the best meteorological and oceanographic data available for each day of radar observations by CSL. The total energy of a (gravity) wave system, per unit area of water surface, is equal to $1/2\ \rho g E$ where ρ is the density of water and g is the acceleration of gravity.

a Standard deviation.

b Does not include samples during rain squall.

c On September 24, both wind speed and wave pole measurements were made in the area over which the plane was being flown. The measured wind speed was 10 K. The wave pole data was used by the Hydrographic Office to derive an energy spectrum from which the wave energy E was calculated to be 0.23 ft^2.

remember that the spectrum has been smoothed over the full 15 second sample. An interval of fifteen seconds represents fifteen patches of sea, each 250 ft. long, under the conditions of the flights or 30 or more ocean waves of average length. The 15 second loops therefore represent adequate samples of the ocean surface.

(b) Qualitative Discussion

The spectra from the rough seas were generally found to be broad and asymmetrical when the radar was looking upwind or downwind. These effects did not appear when the radar was looking crosswind. An example of an asymmetrical spectrum may be seen in Plate II, Sample No. 140. The scatterers that were responsible for the broadened (or less steep) side of the spectrum always moved downwind, as had been observed[2] in our Key West experiments.* The degree of asymmetry and bandwidth of the spectrum increase with the roughness of the sea. We have not tried to analyze the correlation of the degree of asymmetry with the sea conditions, but we shall later indicate the correlation of the bandwidth of the spectrum with sea state variables. The whitecap density as observed visually from the aircraft varied considerably on the different flights and correlates qualitatively with the bandwidth and asymmetries observed. In particular, the whitecap density and clutter bandwidth observed on September 22 were greater than on September 23.

The asymmetry of the clutter spectrum cannot be accounted for by any Gaussian sea surface. There is however other

---

* Note also the ragged downwind edge of the "B" displays in Plate I, Sample Nos. 232 and 300.

experimental evidence for the asymmetry of wave structure on the sea surface. Thus an up- and down-wind skewness of the surface slope distribution has been observed[5] which increases with increasing wind speed. We have tended to interpret the asymmetry of the coherent clutter spectrum as being due entirely to the particle motions of the whitecaps or of the water associated with them, but there may still be some asymmetry of the spectrum owing to asymmetrical distribution and velocity of the scatterers not directly associated with whitecaps.

(c) Empirical Correlation of Clutter Width and Sea State Variables

We have studied several methods of correlating the observed clutter bandwidth* Δ_o and the sea state variables listed in Table I.** The most successful method of correlation involves the observed value of significant wave height $H_{1/3}$ and a period T_m that corresponds to the maximum of the energy spectrum of fully developed ocean waves.***

---

5 Cox and Munk, J. Mar. Research 13, 198 (1954).

* The value of Δ_o quoted here and in Table I is for a constant depression angle of four degrees and represents the average in range of about 15 successive patches.

** The observed bandwidth for September 7 (average of 3 samples) may be in error. It is contradictory to most of our other observations that there could be such a small bandwidth either for a wind speed of 15 knots or for a wave energy of 4 ft^2. The bandwidth for this day is smaller by 40 o/o than the value which would be calculated from Eq. 1. Such narrow clutter bandwidth has been observed otherwise only for low sea states, as for September 16 or some of the Key West data. We therefore omitted it in making the final correlation described by Eq. 1.

*** Let $A^2(f)\,df$ be the contribution to the wave energy by waves in the frequency range f to f + df. If the maximum of the function $A^2(f)$ occurs at $f = f_m$, then $T_m = f_m^{-1}$.

The period T_m is derived from the hindcast wave energy E using Fig. 2.9a of a report[6] of the Hydrographic Office. The correlation that was found in our data* is expressed by the equation

$$\Delta_o = D\, H_{1/3} / T_m \qquad (1)$$

where the dimensionless factor D was determined from the experimental data and was found to be equal to 11 ± 1; Δ_o is expressed in velocity units; and $H_{1/3}$ and T_m are in units that are consistent with those of Δ_o. It must be remembered that all of the sea state quantities, E, $H_{1/3}$, and V_a, the wind speed, are somewhat uncertain and to an extent that it is difficult to estimate.

Deviations from Eq. 1 correlate somewhat with the wind speed or with the state of development of the sea. Thus D is possibly equal to 10 for undeveloped seas or for low wind speeds, and possibly equal to 12 for fully developed or decaying seas or for high wind speeds. Table I does not contain enough data to verify these possibilities with any certainty. The experimental data fits Eq. 1 slightly better when T_m is derived from E than when it is derived from the wind speed or from the observed significant wave height. It may be remarked that the bandwidth Δ_o is proportional to wind speed within about 14 o/o, excepting again the data for September 7, but

---

6 U. S. Navy Hydr. Off. Publ. No. 603 (1955).

* The data used includes all runs in Table I except the run on September 7 and the crosswind run on September 25.

the deviations from this correlation do not themselves correlate with the state of the sea or with any other parameter listed in Table I. This is not surprising if we remember that it is the strength of the sea return rather than its bandwidth that we should expect to correlate with the wind speed.* The apparent density of white caps, which can be estimated from aerial photographs of the sea, also correlates better with bandwidth than does the wind speed.

The good correlation found between Δ_o, $H_{1/3}$ and T_m is rather surprising in view of the fact that white caps apparently contribute to the asymmetric broadening of the spectrum but that as yet no quantitative correlations between white cap properties and more familiar sea state parameters such as the wave energy are known. The theoretical description of white capping has been begun in a limited way[7], (See Sect. II: 6, 9.2, 9.3) but experimental studies of white cap phenomena are needed before the theory can be advanced appreciably.

Our use of the observed wave energy E to derive the value of T_m, the period of maximum spectral energy, is open to criticism since we are using a graph which is based on a spectrum which is probably dimensionally unsound.[8] However, the slight change in the nature of the Neumann-Pierson spectrum needed to make this spectrum dimensionally

---

* Dimensionless groups tried that did not yield good correlation were $\Delta_o^2/g\sqrt{E}$, $\Delta_o^2/g\,H_{1/3}$, $\Delta_o\,T_m^{(E)}/H_{1/3}^{(E)}$, and $\Delta_o V_a/g\sqrt{E}$, all factors having the observed values except $H_{1/3}$ and $T_m^{(E)}$ which were calculated from the observed values of E.

7 CSL Report R-83 (1956).

8 Private communication from Prof. O. M. Phillips.

correct produces only a 12 o/o change in the value of T_m derived from E and in the proportionality constant in Eq. 1. The form of the equation would not thereby be changed. A more serious error may be involved in applying Pierson's spectrum for a fully developed sea to our data which does not always correspond to the fully developed situation.

(d) The Variation of Bandwidth with Depression Angle

Our data seem to show that there is a variation of coherent clutter bandwidth Δ_o with depression angle θ of the radar for some experimental conditions and not for others. This variation can be described conveniently as the increase δ in Δ_o when θ changes from 1^o to 10^o. For crosswind observation, $\delta = (40 \pm 15)$ cps. for the medium sea state conditions of Run No. 9. For the high sea state of Run No. 6, the upwind value of δ is (35 ± 15) cps. and the downwind value appears to be (-120 ± 40) cps.! Although the downwind value is derived from bandwidth data for depression angles in the limited range of $2.5 - 6^o$, the data does seem to require the conclusion that for this case, as the depression angle is increased the bandwidth is decreased, a surprising result which requires further experiments before it is to be understood. For all runs other than No. 6 and No. 9, there appears to be, at most, a small change of Δ with θ, corresponding to the expression $\delta = 20 \pm 20$ cps. The narrow bandwidth found at 1.3^o and sea state 1 in the Key West experiments[2] is not in disagreement with the Quonset data.

3. Comparison with Theory

In order to discuss the possibility of making a quantitative comparison with the theory, we assume now that we may interpret the coherent clutter spectrum as a probability distribution of the velocity of the scatterers. The one-half power points on the clutter spectrum then correspond to those points on the probability distribution where the curve has reached one-half of the value at the maximum. The validity of this interpretation cannot be tested until much more refined experimental data, both radar and oceanographic, become available. For this interpretation to be correct, it is sufficient, but not necessary, that the scatterers are independent; that the effect of the finite lifetime of the scatterers can be neglected; and that there are no shadowing or interference effects.* We assume further that it is only the particle velocities of scatterers that is sensed by the coherent radar and not the configuration velocities.** On the basis of these assumptions, we say that there are several possible contributions to the width of the probability distribution of particle velocity (or to the equivalent coherent clutter bandwidth):

---

* For depression angles of a few degrees, it is probable that shadowing and interference will affect the energy backscattered in each doppler frequency bin.

** We are using the term <u>particle</u> velocity here to refer to the first order, circular motion of the particles of water. We consider the drift and second order velocities later. Examples of <u>configuration</u> velocities are the velocity of propagation of the phase of a sinusoidal wave, or of a hump, a hollow, a "facet", etc. of a random surface.

(i) The distribution of particle velocities of the "solid" water. The scatterers, which here are the small waves, ride on the larger waves. The velocity of the scatterers therefore is the particle velocity of the larger waves.

(ii) The distribution of drift velocities of the "solid" water. Few oceanographic measurements are available of this wave characteristic and no quantitative correlation with sea state parameters has been made. It is probable that the r.m.s. value of that part of the drift velocity owing to the non-linear superposition of the water waves is smaller than the r.m.s. particle velocity by at least a factor of 3. The shearing action of the wind also produces a drift which is probably somewhat larger. Thus the Key West coherent radar measurements indicated that a spread of drift velocities of as much as two knots was possible, and this is not in contradiction with qualitative observations of drift velocities at sea.

(iii) The distribution of particle velocities of breaking wave crests, of spray drops, filaments and perhaps foam patches associated with whitecapping. No calculations or measurements are available here except for the small amount of data obtained[2] from the Key West measurements which indicated that, in the area that was observed, the width of the white cap velocity distribution was about three knots and that the most probable velocity of white cap material was 2 to 3 knots downwind relative to the most probable velocity of the wavelets.

It is therefore possible to make quantitative calculations based on specific models of the ocean surface only for the so-called

particle velocities of the "solid" water, and these calculations can be expected to yield only part of the observed width of the velocity distribution. Two types of calculations relating to the particle velocity of the "solid" water will be mentioned. One calculation yields the width at half probability of the distribution of the component of particle velocities in the direction of the wind. This width is also equal to the bandwidth of the clutter, Δ_o, if we ignore the variation of width with depression angle. The other calculation yields the ratio of cross-wind and up-down-wind half-widths.

The clutter bandwidth Δ_o was computed for several wave spectra and for several uses of the sea state data as given in Table 1. For example, one can assume the Neumann-Pierson wave spectrum for a fully developed sea and then use the observed value either of E, $H_{1/3}$ or V_a to calculate the bandwidth. Such various calculations produce a wide spread of values of Δ_o, including the experimentally observed bandwidth. Note however that for our data, the sea was not always fully developed and the relation $H_{1/3}\, E^{-1/2} = 2.83$ was seldom satisfied.

For purposes of orientation it is worthwhile quoting one formula for Δ_o. This formula is derived on the basis of the following assumptions:

(i) The form of the Neumann-Pierson wave spectrum[9] for a fully developed sea is correct.

---

9 Advances in Geophysics, Vol. 2, p. 93. Academic Press (1955).

(ii) The azimuthal variation of (wave) spectral energy is such that $\sigma_u^2 = 0.866\ \sigma_w^2$ where σ_u^2, σ_w^2 are the variances of the components of orbital particle velocity in the direction of the wind and along the vertical, respectively.

On this basis we can show that

$$\Delta_o = 4.5\ H_{1/3}/T_m \qquad (2)$$

where, as before, T_m is the period corresponding to the maximum of the energy spectrum plotted against frequency.

This result suggests that, at most, less than one-half of the clutter bandwidth has its origin in the spread of orbital particle velocities of the waves and the remainder comes from the spread of drift velocities and of the velocities associated with whitecapping.

We have but one check point for this equation. Wave staff measurements obtained on September 24 yielded a wave spectrum from which we computed directly $E = 0.23\ ft^2$ and $\Delta_o = 0.62K$. This energy of the wave system is fully developed, as comparison of the observed values of E, $H_{1/3}$ and V_a with Pierson's charts will show. The distribution of energy over the wave spectrum is not characteristic of the wind speed however, for there were strong components for periods in excess of eight seconds. These low frequency components contribute to E and $H_{1/3}$ but not to the value 0.62 of Δ_o computed from the observed wave spectrum. The value of Δ_o computed from Eq. 2 is 1.2K and the value observed was 2.47K. In this case it appears that only one quarter of the observed bandwidth can be attributed to the orbital motion of the waves.

It is clear that much more detailed oceanographic data is necessary before the correct description of sea surface is known from which even the orbital particle velocity distribution can be computed with some certainty.

For that part of the sea surface that can be described by a Gaussian random process, a relationship of the form

$$\sigma_w = \pi(2E)^{1/2} / \tilde{\bar{T}} \qquad (3)$$

should hold irrespective of the nature of the energy spectrum of the waves. In this equation, $\tilde{\bar{T}}$ is the average time between zero up-crossings and σ_w^2 is the variance of the vertical component of the particle velocity of the waves. For the Neumann-Pierson spectrum, Eqs. 2 and 3 are equivalent. Eq. 1 is somewhat similar to Eq. 3 but $E^{1/2}$ has replaced the approximately proportional quantity $H_{1/3}$ and $\tilde{\bar{T}}$ has replaced T_m. Simultaneous observation at sea of $\tilde{\bar{T}}$, σ_w, and E would to some extent show whether the ocean surface is stationary and Gaussian as is usually assumed.

We have little data to compare with the theoretical predictions of clutter widths for cross-wind as compared to the up- and down-wind direction of observation. The $\cos^2$ dependence of the wave spectrum on azimuthal angles suggested by Pierson should give a ratio of clutter bandwidths for the cross-wind and the down-wind directions equal to 0.58. The value observed (Flight 9) was 0.78 ± 0.15. This significantly higher value corresponds to a wider beamwidth, that is to shorter crests, than the $\cos^2$ law would predict.

In the future, more careful comparison should be made between bandwidths or particle velocities observed by coherent radars and those predicted from theoretical wave spectra. Wherever possible a measured wave spectrum should be used rather than one which assumes that the sea is fully developed or that the angular distribution follows the $\cos^2$ law. Furthermore, account should be taken of the fact that measurements obtained from airborne observation essentially sample in distance more nearly than in time.

4. Some Anomalies

In five of the two hundred sea clutter samples the "B" display indicated an interesting anomaly. Examples of this are shown in Plate II, Sample Nos. 171 and 267.* Here we see that a short interval of the display has a spectrum which is greatly shifted from the main part. This occurred twice on the flight of September 22, twice on the flight of September 23, and once on the flight of September 24. The areas where these occurred are marked with an asterisk (*) in the map of Fig. 1. Neither hydrographic maps nor visual observations from the aircraft indicated any obvious cause of this phenomenon (e.g. shoals). For the five anomalous samples the average shift from the center of the displaced spectrum to the center of the normal spectrum is approximately 225 cycles per second corresponding to 7 knots and the duration of the displaced spectrum is one

---

* We note that the "tails" of the "A" displays, for these anomalous cases and for the cases where f-ming occurred, are artifacts that have no immediately useful interpretation.

to two seconds. In all cases the displacement was down-wind. A violent gust blowing in the direction of the mean wind might produce this displaced clutter if it roughened the water over a sufficiently large area and increased its drift velocity, on the average, by 7 knots, or if it produced an unusually large and rapidly moving volume of white cap spray. A school of fish breaking water or a flight of sea birds might also have been the source of what appeared to be displaced clutter.

Another effect noticed several times was a sudden increase in the spectrum intensity over an area approximately 700 ft. in length. This effect occurred on calm days without any shift but with some broadening of the spectrum and may very well represent the effect of a gust blowing across the mean wind direction.

During the course of one of the flights the radar return from a rain squall was clearly visible on the output of Rayspan and was recorded on tape and analyzed in the laboratory. The results indicate that the rain clutter bandwidth was 2.5 knots, was wider than that of the sea by about 50 o/o, and was displaced from it in the wind direction by 6 knots. The wind velocity from the hindcast data was 8 knots giving a 5.5 knot component in the direction of the antenna azimuth. Some "A" and "B" spectra displays of the squall may be seen in Plate III, Samples 11A and 108. It should be noted that the rain clutter comes from a volume whose bounds are determined by the range gate, the azimuth and the elevation beam patterns of the antenna, and the sea surface.

AUTHORIZED DISTRIBUTION LIST

As of June 20, 1958

Number of Copies	Agency
	Director of Research and Development Headquarters United States Air Force Washington 25, D. C.
1	Attn: AFDRD-AC/2
1	AFDRD-CC/2
1	Commander Headquarters, Air Research and Development Command P. O. Box 1395 Baltimore 3, Maryland Attn: RDDDR-5
1	Headquarters, Air Force Office of Scientific Research Air Research and Development Command United State Air Force Washington 25, D. C. Attn: SROP
1	Commander Air Force Cambridge Research Center Laurence G. Hanscom Field Bedford, Massachusetts Attn: CRR
	Commander Wright Air Development Center Wright-Patterson Air Force Base, Ohio
2	Attn: WCOSI-3
1	WCLG
1	WCRR
1	WCLR
1	WCLOT-2 (Mr. Cooper)
2	WCLRW (Mr. Clute)
1	Commander United States Air Force Security Service San Antonio, Texas Attn: CLR
1	Commanding Officer Rome Air Development Center Griffiss Air Force Base, New York

Number of Copies	Agency
1	Director Air University Library Maxwell Air Force Base, Alabama Attn: CR-4803a
1	Commander Air Force Armament Center Eglin Air Force Base, Florida Attn: Deputy for Operations
	Chief, Bureau of Ships Department of the Navy Washington 25, D. C.
2	Attn: Code 280
1	Code 565C
1	Code 810
1	Code 810B
1	Code 812
1	Code 820
1	Code 825
1	Code 830
1	Code 835
	Chief, Bureau of Aeronautics Department of the Navy Washington 25, D. C.
1	Attn: EL-402
1	TD-4
	Department of the Navy Office of Naval Research Washington 25, D. C.
1	Attn: Code 900
1	Code 430
2	Code 437
1	Commanding Officer Office of Naval Research Chicago Branch John Crerar Library Building 10th Floor, 86 East Randolph Street Chicago 1, Illinois
1	Bureau of Ordnance Department of the Navy Washington 25, D. C. Attn: Re4C

Number of Copies	Agency
1	Director Office of Naval Research Branch Office 1000 Geary Street San Francisco, California
2 (Progress Reports only)	U. S. Navy Inspector of Ordnance Applied Physics Laboratory The Johns Hopkins University 8621 Georgia Avenue Silver Springs, Maryland
	Commanding Officer and Director U. S. Naval Electronics Laboratory San Diego 52, California
1	Attn: Library
1	Code 2800, C. S. Manning
	Director Naval Research Laboratory Washington 25, D. C.
3	Attn: Code 5140
	Chief of Naval Operations Navy Department Washington 25, D. C.
1	Attn: OP-51
1	OP-371-C
1	OP-551
1	OP-345
1	Commanding Officer Naval Air Development Center Johnsville, Pennsylvania Attn: Code AAEL
1	Commander Naval Ordnance Laboratory White Oaks Silver Springs 19, Maryland Attn: Technical Library
1	Head, Combat Direction Systems Branch (OP-345) Department of the Navy Room 4C-518 Pentagon Washington 25, D. C.

Number of Copies	Agency
	Department of the Army Office of the Chief Signal Officer Washington 25, D. C.
1	Attn: SIGRD
1	SIGRD-9-b
1	Chief of Research and Development Office of the Chief of Staff Department of the Army Washington 25, D. C.
1	Assistant Chief of Staff, Development and Test Headquarters, Continental Army Command Fort Monroe, Virginia
1	President, U. S. Army Airborne and Electronics Board Continental Army Command Fort Bragg, North Carolina
1	President, U. S. Army Defense Board Continental Army Command Fort Bliss, Texas
	Office of the Chief of Ordnance Department of Ordnance Washington 25, D. C.
1	Attn: ORDTR
1	ORDTB
2	Commanding General Redstone Arsenal Huntsville, Alabama Attn: Technical Library
1	Commanding Officer Office of Ordnance Research 2127 Myrtle Drive Duke Station Durham, North Carolina
3	Director Ballistics Research Laboratory Aberdeen Proving Ground, Maryland Attn: Dr. L. A. Delsasso
1	Commanding Officer Frankford Arsenal Philadelphia 37, Pennsylvania

Number of Copies	Agency
1	9560 S. C. Electronics Research Unit P. O. Box 205 Mountain View, California
20	Transportation Officer Fort Monmouth Little Silver, New Jersey Marked for: SCEL Accountable Property Officer Building 2700 Camp Wood Area Inspect at Destination File No. 0060-PH-54-91(5308)
1	Director National Bureau of Standards Washington 25, D. C. Attn: Dr. S. N. Alexander
1	Librarian Instrumentation Laboratory Massachusetts Institute of Technology Cambridge 39, Massachusetts
1	Director Jet Propulsion Laboratory California Institute of Technology Pasadena, California
1	Chicago Midway Labs 6040 South Greenwood Avenue Chicago 37, Illinois Attn: Librarian
1	Hughes Research and Development Library Hughes Aircraft Company Culver City, California Attn: Miss Mary Jo Case
1	Mr. Robert R. Everett Division Head Lincoln Laboratory Massachusetts Institute of Technology Lexington 73, Massachusetts
1	Technical Documents Service Willow Run Laboratories University of Michigan Willow Run Airport Ypsilanti, Michigan

Number of Copies	Agency
1	The Rand Corporation 1700 Main Street Santa Monica, California Attn: Library
1	Dr. C. C. Furnas Cornell Aeronautical Laboratory Buffalo, New York
1	Massachusetts Institute of Technology Lincoln Laboratory P. O. Box 73 Lexington 73, Massachusetts
1	W. L. Maxson Corporation 460 West 34th Street New York 1, New York
1	Stanford University Electronics Research Laboratory Stanford, California
1	Radio Corporation of America RCA Laboratories Division David Sarnoff Research Center Princeton, New Jersey Attn: Mr. A. W. Vance
1	The Johns Hopkins University Operations Research Office 6410 Connecticut Avenue Chevy Chase, Maryland For: Contract DA 44-109 qm-266
1	Light Military Electronic Equipment Department General Electric Company French Road Utica, New York For: Contract AF 33(600)-16934
1	Goodyear Aircraft Corporation Akron 15, Ohio For: Project MX 778 Contract W33-038 ac-14153
1	Mr. A. A. Lundstrom Bell Telephone Laboratories Whippany, New Jersey

Number of Copies	Agency
10	Armed Services Technical Information Agency Arlington Hall Station Arlington 12, Virginia
1	Litton Industries 336 North Foothill Road Beverly Hills, California Via: Inspector of Naval Materiel Los Angeles, California
1	Remington Rand Univac Division of Sperry Rand Corporation Via: Insmat, BuShips Insp. Officer 1902 West Minnehaha Avenue St. Paul 4, Minnesota
1	Technical Library Code 142 David Taylor Model Basin Washington 7, D. C.
1	Commanding Officer and Director David Taylor Model Basin Washington 7, D. C. Attn: Code 800
1	Naval Ordnance Proving Ground Computation Center Dahlgren, Virginia Attn: R. A. Niemann
1	System Development Corporation 2500 Colorado Avenue Santa Monica, California
5 (Progress Reports only)	National Advisory Committee for Aeronautics 1512 H Street Northwest Washington 25, D. C.